Resonance Raman scattering in Cr^{4+}-doped forsterite

Dana M. Calistru, W. B. Wang, V. Petričević, and R. R. Alfano
Institute for Ultrafast Spectroscopy and Lasers,
New York State Center of Advanced Technology for Ultrafast Photonic Materials and Applications,
Physics Depatment, The City College and Graduate School of the City University of New York,
138th Street & Convent Avenue, New York, New York 10031
(Received 30 November 1994; revised manuscript received 30 January 1995)

Seven Cr^{4+} vibronic modes were obtained by means of resonance Raman scattering. These modes were measured at 253, 290, 480, 498, 690, 740, and 764 cm^{-1} in Cr^{4+}:Mg_2SiO_4. The symmetry of each of the modes was established and correlated to the molecular symmetry (T_d). The effective force constants for the Si-O and Cr^{4+}-O bonds were estimated where a decrease of $\approx$13 to 29% (model dependent) was found when Cr^{4+} substitutes for Si. Possible energy matching between vibronic and host phonon modes are suggested as nonradiative pathway.

I. INTRODUCTION

The overall properties of solid-state tunable lasers are largely affected by nonradiative relaxation processes which are considered to be the main loss channel in such materials. Recently, several attempts were made to understand which vibronic (impurity associated) and phonon (lattice) modes are involved in nonradiative processes present in impurity doped dielectric crystals.[1] The criteria concerning which host (lattice) and impurity ions should be considered for obtaining an efficient laser system is still under study and not sufficiently understood. The present study is concerned with chromium doped forsterite (Cr:Mg_2SiO_4), a new tunable solid-state system operating in the near-infrared region, developed by Alfano and co-workers,[2,3] in which Cr^{4+} placed in a tetrahedral site has been identified as laser-active ion.[2,4,5] Cr enters this host with two oxidation states: Cr^{3+} and Cr^{4+}. Cr^{3+} is favored by a reducing growing atmosphere, while Cr^{4+} is favored by an oxidized atmosphere.[3,6] Cr^{4+} substitutes for Si which has T_d molecular symmetry and occupies a position with C_s site symmetry. Cr^{3+} substitutes for Mg which occupies two distinct octahedral coordinated crystallographic positions. One has C_i site symmetry [Mg(I)] and the other one has C_s site symmetry [Mg(II)]. Several other hosts having the same laser-active ion with the same molecular symmetry (T_d) have been tried unsuccessfully. Laser operation of Cr^{4+}:Y_2SiO_5 and Cr^{4+}:$LiNbGeO_5$ have been reported[7] but their operation above 77 K is severely affected by nonradiative processes. One step in understanding nonradiative processes is to study the phonon and vibronic modes and their interactions.

Photoexcitation of an impurity ion can be allowed either by radiative deexcitation, which is sometimes accompanied by phonon emission, or by energy transfer from the hot ion into the lattice through nonradiative processes. In the latter case the hot ion's vibronic modes couple with (some) phonon modes and enable energy dissipation into the lattice. When this coupling is strong the overall lasing properties are significantly altered, if not destroyed. Up to this date, there is no theory to predict which phonon and vibronic modes are involved in nonradiative processes in laser action and what are the most important features which determine their coupling.

One of the necessary, but not sufficient conditions for phonon-vibronic mode coupling is the energetic one; another is the symmetry. Rebane[8] distinguishes two cases:

(a) the vibronic frequency lies in one of the allowed bands of the ideal crystal and is in resonance with certain phonon modes. Such a mode is called a "band vibration"; and

(b) the vibronic frequency lies in one of the forbidden bands of the ideal crystal. There can be no resonance with any phonon mode; such a mode is called a "localized vibration." There is yet another class of vibrations—"pseudolocalized vibrations" which are, in fact, band vibrations but coupling with phonon modes is very weak. It will be shown that in Cr^{4+}:Mg_2SiO_4 no localized vibrations can appear.

In the past, limited experimental and theoretical studies have been pursued. Ultrafast spectroscopy offers a direct tool for investigating nonradiative processes in solid-state systems. The pump-and-probe time-resolved technique has revealed the participation of the 225, 335, and 370 cm^{-1} phonon modes[1] in the nonradiative relaxation of Cr^{4+}:Mg_2SiO_4.

This paper investigates the Cr^{4+} vibronic modes in Cr-doped Mg_2SiO_4 and their potential interaction with the host phonon modes, i.e., participation in nonradiative processes. The first-order resonance Raman spectra of Cr^{4+} due to the $^3A_2 \rightarrow {}^3B_2$ ($^3T_1$) transition will be discussed and compared with previous data. Undoped forsterite (which is transparent in the considered spectral region) was used as a reference material for identifying the resonance-enhanced modes in Cr^{4+}:Mg_2SiO_4.

II. CRYSTAL STRUCTURE

The host crystal is forsterite, Mg_2SiO_4, which belongs to the olivine family. Its space group is D_{2h}^{16} in the

Schoenflies notation and has four molecules (i.e., 28 atoms) per unit cell.[9] Six different crystal notations have been used for this material (*Pnma*, *Pbnm*, *Pmcn*, *Pnam*, *Pnmb*, and *Pcmn* according to the choice of axis).[10] Laser and spectroscopic studies have mainly used the *Pbnm* and *Pmnb* notations, while vibrational analysis studies have used both the *Pnma* and *Pbnm* notations. Previous work done by our group on forsterite laser has used the *Pbnm* notation. In Table I, the correlation between the *Pnma*, *Pbnm*, and *Pmnb* notations and the crystal's lattice constants are presented.

Throughout this study the *Pnma* notation will be used. In the *Pnma* notation the lattice constants are $a=10.22$ Å, $b=5.99$ Å, and $c=4.76$ Å and are identified with the x, y, and z axes, respectively. Although Devarajan and Funck[9] clarified the confusions made between the *Pnma* and the *Pbnm* notations, as well as the correspondence between them, mistakes were still made. It should be noted that although Iishi[11] was used as a reference paper by many authors, it presents the experimental data in *Pbnm* notation, but the irreducible representation in *Pnma*.

In *Pnma* notation the irreducible representation for the Mg_2SiO_4 optical-phonon modes is[9]

$$\Gamma=11A_g+7B_{1g}+11B_{2g}+7B_{3g}+10A_u+14B_{1u}+10B_{2u}+14B_{3u}\ .$$

Only the even ($A_g, B_{1g}, B_{2g}, B_{3g}$) representations are Raman active. The appropriate scattering geometries for these representations are used in our experiments.

III. EXPERIMENTAL METHOD

The experimental setup used in our work consists of a CW mode-locked Nd:YAG laser (≈ 7 W output power), with a repetition rate of 82 MHz, a synchronously pumped Rh-6G dye laser, a triplemate SPEX spectrograph, and a photon counting system. The dye laser was tuned to 575 nm (the maximum of absorption for Cr^{4+}:Mg_2SiO_4, for $E_i \| c$). The sample was irradiated with $a \approx 10$ mW beam focused to a diameter of ≈ 20 μm. The Raman spectra were recorded in a 90° scattering arrangement, at room temperature with a SPEX triplemate spectrograph with a resolution of ≈ 5 cm^{-1} and a photon counting image acquisition system (PIAS, Hamamatsu, model C1815). The samples were an undoped $15\times12\times5$ mm-oriented Mg_2SiO_4 single crystal, which was used as reference medium and a Cr^{4+}:Mg_2SiO_4 $10\times8\times6$ mm-oriented single crystal, with the concentration of Cr^{4+} estimated at $N\approx3\times10^{18}$ ions/cm^3. Both crystals were free from visible inhomogeneities such as inclusions, cracks or bubbles.

TABLE I. Correlation between the *Pnma*, *Pbnm*, and *Pmnb* notations and the crystal's lattice constants (Ref. 10).

Lattice constants (Å)	*Pnma*	*Pbnm*	*Pmnb*
10.22	*a*	*b*	*b*
5.99	*b*	*c*	*a*
4.76	*c*	*a*	*c*

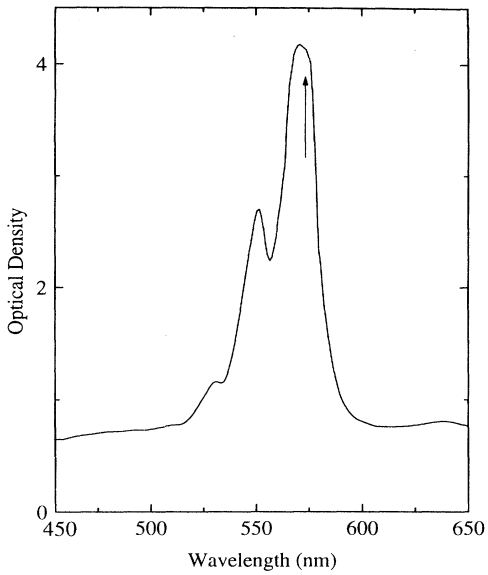

FIG. 1. Polarized absorption spectra for Cr:Mg_2SiO_4, $E\|c$, at room temperature. Arrow position indicates excitation wavelength ($\lambda_0=575$ nm) used for obtaining resonance Raman spectra in Figs. 2 and 3.

The absorption spectra at room temperature for Cr:Mg_2SiO_4, with the incident polarized light (E_i) parallel to the c axis ($E_i \| c$) is given in Fig. 1. Although both Cr^{3+} and Cr^{4+} contribute to the overall absorption, the site-selective excitation spectra[5] show that the absorption structure in the 575 nm region is due entirely to Cr^{4+} (Cr^{3+} has a minimum of absorption in this region). Mg_2SiO_4 is transparent in this spectral region. The resonance-enhanced Cr^{4+} Raman lines were obtained at the exciting wavelength $\lambda_0=575$ nm, ($E_i \| c$) which corresponds to the dipole allowed transition $^3A_2 \rightarrow {}^3B_2(^3T_1)$. $^3T_1$ is the Cr^{4+} state in T_d symmetry. As Cr substitutes for Si which has C_s site symmetry, an orthorhombic distortion has to be considered. $^3B_2$ is the excited-state symmetry corresponding to the 575 nm transition in a C_{2v} configuration (as approximation for C_s).[5]

IV. VIBRATIONAL ANALYSIS

As Cr^{4+} has T_d molecular symmetry, with four oxygen atoms surrounding it, it has nine normal modes of vibration distributed among the irreducible representations of T_d in the following manner:

$$\Gamma=A_1+E+2T_2\ .$$

The molecular symmetry will be reduced by the site symmetry C_s. Further on, by standard group-theoretical methods, C_s is correlated to the crystal's space group D_{2h}. These correlations are summarized in Table II.

We expect six totally symmetric resonance-enhanced modes which should be observed in the A_g and/or B_{2g}

TABLE II. Molecular, site, and space-group symmetry correlations (Ref. 12) for Cr^{4+} in Mg_2SiO_4 and the expected number and symmetry of vibronic Cr^{4+} associated modes. The degeneracy of each mode is indicated in parentheses in columns 1, 2, and 3.

T_d (molecular symmetry)	C_s (site symmetry)	D_{2h} (space-group symmetry)	Number of totally symmetric modes	Number of nontotally symmetric modes
$A_1(1)$	$A'(1)$	$A_g(1), B_{2g}(1)$	1	0
$E(2)$	A'	A_g, B_{2g}	1	0
	$A''(1)$	$B_{1g}(1), B_{3g}(1)$	0	1
	A'	A_g, B_{2g}	1	0
$T_2(3)$	A'	A_g, B_{2g}	1	0
	A''	B_{1g}, B_{3g}	0	1
	A'	A_g, B_{2g}	1	0
$T_2(3)$	A'	A_g, B_{2g}	1	0
	A''	B_{1g}, B_{3g}	0	1
			6	3

space-group symmetry (having as basis x^2, y^2, z^2, and xz, respectively) and three nontotally symmetric modes observable in B_{1g} and/or B_{3g} space-group symmetry (having as basis xy and yz, respectively).[12]

It should be mentioned that resonance-enhanced modes can not be observed in the B_{1g} symmetry since B_{1g} has as basis xy and in order to have absorption (i.e., resonance conditions) at 575 nm, the polarization of the incident light has to be along the z (c) axis.

V. EXPERIMENTAL RESULTS

The Stokes Raman spectra at room temperature for Cr^{4+}:Mg_2SiO_4 and undoped Mg_2SiO_4 are shown in Figs. 2 and 3. Figure 2 presents the resonance-enhanced modes obtained in the A_g symmetry, for different spectral ranges. The position of these modes is 253, 290, 498, 690, and 764 cm^{-1}. Figure 3(a) presents the only resonance-enhanced mode detected in the B_{2g} symmetry: 690 cm^{-1}. Figures 3(b) and 3(c) present the resonance-enhanced modes obtained in the B_{3g} symmetry: 480 and 740 cm^{-1}. No other resonance-enhanced modes were detected outside of the spectral ranges shown in Figs. 2 and 3. Table III summarizes the results presented in Figs. 2 and 3. The estimated accuracy of the measured frequency for the vibronic modes was $\approx \pm 3$ cm^{-1}.

VI. DISCUSSION

A. Missing modes

Instead of the expected six resonance-enhanced totally symmetric modes and the three nontotally symmetric modes only five and two were observed, respectively. The total intensity of the resonance Raman spectrum is proportional to the sum of the A and B terms described below, provided that a nonperturbed ground state is considered. According to Albrecht's theory[13] the resonance-enhanced totally symmetric modes correspond to configurations with large Franck-Condon overlap integrals and are given by the A term:[14]

$$A=\sum_{e\neq g}\sum_{\nu}\frac{[g_0|R_\sigma|e_0][e_0|R_\rho|g_0](i|\nu)(\nu|j)}{h(\nu_{ev}-\nu_{gi}-\nu_0)-i\Gamma_e}, \quad (1)$$

where $|g_0]$ and $|e_0]$ are the nonperturbed ground, and excited electronic states, respectively, R_σ and R_ρ the transition moments, $|i)$, $|\nu)$, $|j)$ the initial, intermediate, and final vibronic states, respectively, $h\nu_{ev}$, $h\nu_{gi}$ the energies in the excited, and ground states, $h\nu_0$ the exciting energy and $i\Gamma_e$ the damping term. Thus for a particular vibronic mode, the A term will be nonzero for a nonzero Franck-Condon overlap. This implies that the minimum of the excited electronic level potential is displaced in coordinate space with respect to the minimum of the ground state (there exists a Stokes shift). Therefore, a possible explanation for the absence of one totally symmetric mode would be that the Stokes shift is small for this particular mode or the oscillation strength is weak.

The mechanism for obtaining nontotally symmetric resonance-enhanced modes is different, and is connected to the B term[14] term by

$$B=\sum_{e\neq g}\sum_{s\neq e}\sum_{\nu}\sum_{a}\frac{[g_0|R_\rho|e_0][e_0|h_a|s_0][s_0|R_\sigma|g_0](i|Q_a|\nu)(\nu|j)}{h(\nu_{e0}-\nu_{s0})[h(\nu_{ev}-\nu_{gi}-\nu_0)-i\Gamma_e]}+\frac{[g_0|R_\sigma|e_0][e_0|h_a|s_0][s_0|R_\rho|g_0](i|\nu)(\nu|Q_a|j)}{[h(\nu_{e0}-\nu_{s0})[h(\nu_{ev}-\nu_{gi}-\nu_0)-i\Gamma_e]}, \quad (2)$$

where $h_a = \sum_a (\partial H_{ev}/\partial Q_a)|_0$ is the vibronic coupling operator, H_{ev} is the Hamiltonian of the interaction between the electronic and vibronic motion and Q_a is the normal coordinate of mode a. The existence of a nontotally symmetric mode requires the presence of a second

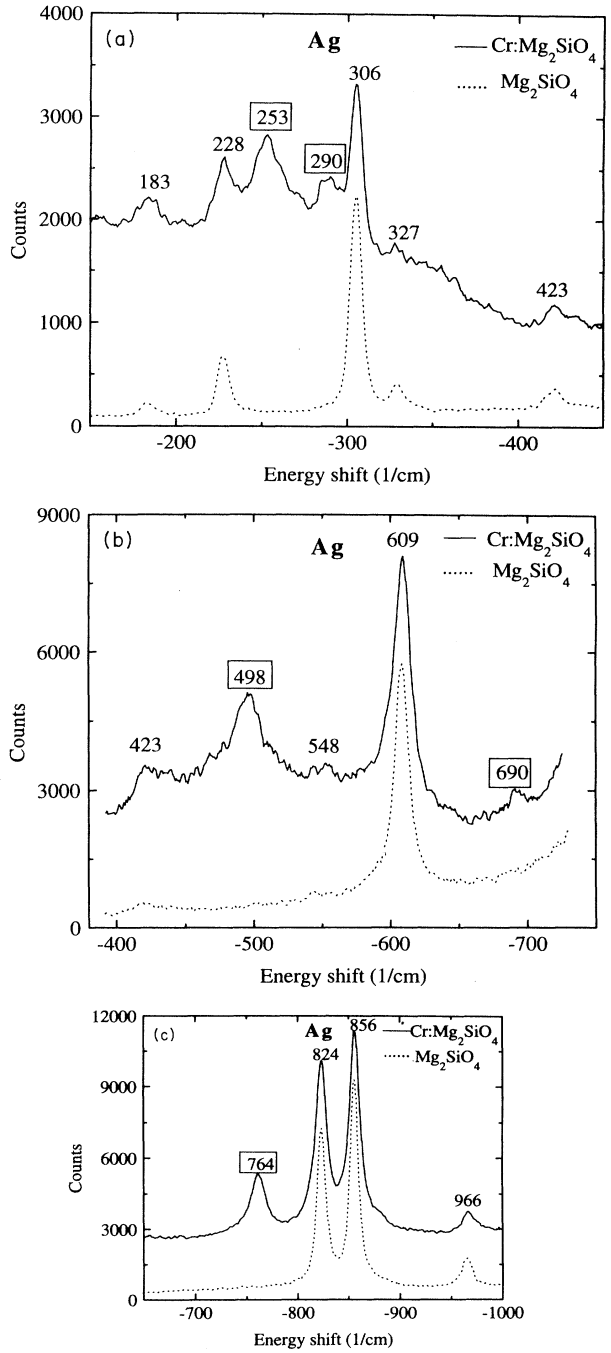

FIG. 2. Polarized Raman (· · · ·) for Mg_2SiO_4 and resonance Raman (——) for Cr^{4+}:Mg_2SiO_4 spectra at room temperature. The intensity of the lines is given in arbitrary units. The scattering configuration is $y(zz)x$, A_g symmetry. The spectral range is (a) 150–425 cm^{-1}, (b) 425–700 cm^{-1}, (c) 700–1000 cm^{-1}. Resonance-enhanced modes are boxed.

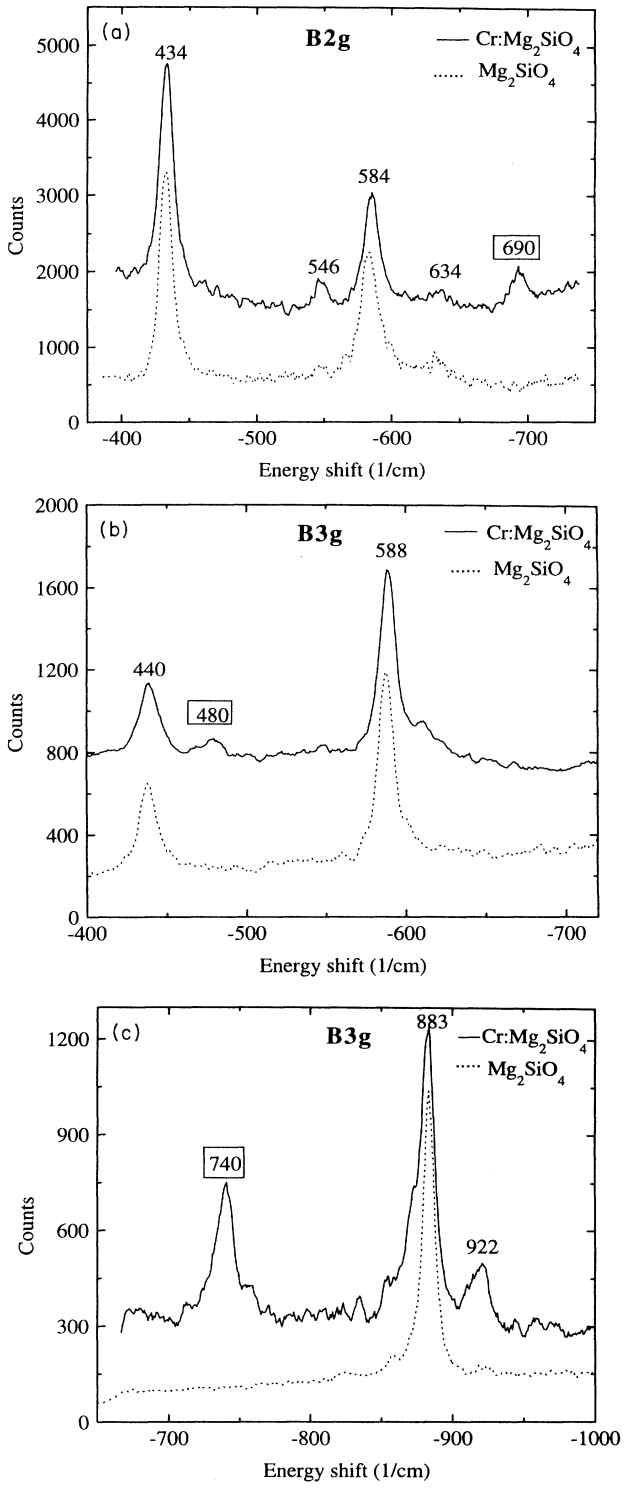

FIG. 3. Polarized Raman (· · · ·) for Mg_2SiO_4 and resonance Raman (——) for Cr^{4+}:Mg_2SiO_4 spectra at room temperature. The intensity of the lines is given in arbitrary units. The scattering configuration is (a) $y(zx)z$, B_{2g} symmetry, 400–700 cm^{-1}, (b) $x(zy)z$, B_{3g} symmetry, 400–700 cm^{-1}, (c) $x(zy)z$, B_{3g} symmetry, 700–1000 cm^{-1} (the 922 cm^{-1} mode leaked from B_{1g} symmetry). Resonance-enhanced modes are boxed.

TABLE III. Frequencies (cm^{-1}) and symmetry assignments (D_{2h}) of the measured resonance enhanced modes of Cr^{4+} in Mg_2SiO_4.

A_g	B_{2g}	B_{3g}
764		
		740
690	690	
498		
		480
290		
253		

excited state $|s_0]$ vibronically coupled (through the vibronic coupling operator h_a) with the excited state $|e_o]$ [$^3B_2(^3T_1)$ in our case]. The absence of one of the three expected nontotally symmetric modes would occur if the above-mentioned coupling term, $[e_0|h_a|s_0]$ is weak or zero.

B. Vibronic assignments

Consideration will be given to the original molecular (T_d) symmetry of the resonance-enhanced modes. In the undoped crystal the frequencies of the four types of T_d modes, denoted as $\nu_1(A_1)$, $\nu_2(E)$, $\nu_3(T_2)$, and $\nu_4(T_2)$ having Si as central ion are in the following ranges:[11] $\nu_3 \in (850-980)$ cm^{-1}, $\nu_1 \in (830-840)$ cm^{-1}, $\nu_4 \in (500-600)$ cm^{-1}, and $\nu_2 \in (420-480)$ cm^{-1}. By taking this ordering into account and the results presented in Tables II and III the following conclusions can be made:

(1) The 764 cm^{-1} mode is the tetrahedral breathing mode $\nu_1(A_1)$. The arguments which support this assignment are (a) the most enhanced modes in resonance Raman experiments are the totally symmetric ones. The 764 cm^{-1} is about ten times more intense than any of the other resonance enhanced modes; (b) although it is not the only totally symmetric mode (taking into account the C_s site symmetry there should be six), it is the only one which originates in a totally symmetric representation in $T_d - A_1$. The other five totally symmetric modes originate in E and T_2 (nontotally symmetric) representations.

(2) The 740 cm^{-1}, 690 cm^{-1} group belongs to $\nu_3(T_2)$. For the complete removal of degeneracy (due to C_S) three distinct modes are expected: two totally symmetric and one nontotally symmetric. Instead, one totally symmetric (690 cm^{-1}) and one nontotally symmetric (740 cm^{-1}) were observed. One totally symmetric mode is missing. Possible explanations have been previously mentioned. It is interesting to remark that the 690 cm^{-1} mode is the only one present in both A_g and B_{2g} representations. This fact supports two possible explanations. The first one is that the 690 cm^{-1} vibration is the same mode in both representations and it merely reflects a high degree of depolarization which is in perfect accordance with its originating in a nontotally symmetric T_d mode as A_g and B_{2g} correspond to the $I_{(\perp)}$ and $I(_{\parallel})$ scattering configurations, respectively. A second explanation is that the 690 cm^{-1} A_g mode is different from the 690 cm^{-1} B_{2g} mode. This could be explained if it is assumed that more than one Cr^{4+} ion is present in each unit cell (which can accommodate up to four Cr ions). Such a situation is not probable if we take into account the low, uniform doping concentration of the sample ($N \approx 3 \times 10^{18}$ ions/cm^3). At the same time, the different positioning inside the unit cell should be reflected by other modes, but is not. All of these arguments suggest that the first explanation is the valid one and we have one totally and one nontotally symmetric mode for $\nu_3(T_2)$.

(3) If 498 and 480 cm^{-1} are assigned to $\nu_4(T_2)$ then 290 and 253 cm^{-1} belong to $\nu_2(E)$. But ν_2 should split into one totally symmetric mode and one nontotally symmetric (see Table II). Thus the only possible assignment remains: 498 and 480 cm^{-1} belong to $\nu_2(E)$, while 290 and 253 cm^{-2} belong to $\nu_4(T_2)$.

C. Calculation of force constants of Si-O and Cr^{4+}-O. Absence of localized modes associated with the Cr^{4+} impurity ions

It was previously stated that for the Cr^{4+}:Mg_2SiO_4 crystal no localized vibrations are expected. The reasoning is as follows: in order for a localized vibration to appear above the highest phonon frequency, quite rigid conditions should be satisfied.[8] The impurity must be lighter by a factor of 1.5–2 than the atom it substitutes for, or there must be an increase in the interatomic force constant between the impurity ion and its nearest neighbor by a factor of 3–5. Cr which substitutes for Si is twice as heavy ($m_{Cr} = 52$ m.u., $m_{Si} = 28$ m.u.). An estimate can be made showing that by substituting Si by Cr^{4+} the effective force constant decreases by $\approx 13-29\%$. Two approximations are used in the estimation:

(i) In the first approximation, by substituting Si with Cr^{4+}, the O-O force constant is assumed not to change. This assumption is based on the fact that due to its low concentration (approximately 1 atom/1100 unit cells) the Cr^{4+} ion is not expected to significantly change the distances inside the tetrahedron (and thus the strength of the bond), which are ultimately determined by the crystal structure.

(ii) In the second approximation, it is assumed that by substituting Si with Cr^{4+} the strength of the covalent bond with O will change. This change should also be reflected in the O-O bond. The second step of this approximation will consider this change. Only the totally symmetric mode $\nu_1(A_1)$ is considered and calculations are made for the T_d and C_{3v} symmetries. C_{3v} is considered to be the effective symmetry induced by the C_s site symmetry. Both changes in Cr^{4+}-O(k_1) and O-O (k_2) force constants are taken into account. The calculations made for T_d symmetry allow the estimate of k_1 and k_2 (for example by using ν_1 and ν_2) and predicts the position of the two remaining modes (ν_3 and ν_4).

1. Estimates for $k_{Si\text{-}O}$ and $k_{Cr\text{-}O}$ for $\nu_1(A_1)$ in T_d and C_{3v} symmetry

The totally symmetric (breathing) mode $\nu_1(A_1)$ is considered under the following assumptions: the problem will be solved only for the unperturbed system (T_d) and

for an effective C_{3v} symmetry induced by the C_s site symmetry; only interactions inside the tetrahedron are taken into account. No other couplings (intertetrahedral, Mg-Si, Mg-O, etc.) are considered; only stretching motions are considered [as calculations are made for $\nu_1(A_1)$].

Using the Lagrange equations, the effective force constant ($k=m\omega^2$, with $m=m_o=16$ m.u.) for the totally symmetric mode $\nu_1(A_1)$ in $T_d(k_{T_d})$ and $C_{3v}(k_{C_{3v}})$ can be written as

$$k_{T_d}=k_1+4k_2\ , \tag{3}$$

$$k_{C_{3v}}=\frac{2k_1+2.4455k_2+3.1563k_3+(5.9805k_2^2+9.9622k_3^2-10.5733k_2k_3)^{1/2}}{2}\ , \tag{4}$$

where k_1 is the Si-O (Cr^{4+}-O) force constant. In Eq. (3), k_2 is the O-O force constant (the same for all four equivalent O atoms in T_d symmetry). In Eq. (4), k_2 and k_3 are the O-O force constants (different for the two groups of nonequivalent O atoms in C_{3v} symmetry).

By considering a mean value[11] of 835 cm^{-1} for the totally symmetric mode in Mg_2SiO_4, an effective force constant $k=6.61$ mdyn/A is obtained. If Cr^{4+} is the central ion, the same mode has a value of 764 cm^{-1} (Table III) which leads to an effective force constant $k=5.54$ mdyn/A. The above equations allow, for the first time, the estimate of the Cr^{4+}-O force constant.

Using Eqs. (3) and (4), the values for k_2 and k_3 from the rigid-ion model[11] (RI) and the measured effective force constant value (k) for SiO_4 and CrO_4, the $k_{1\ \mathrm{Si\text{-}O}}$ and $k_{1\ \mathrm{Cr\text{-}O}}$ force constants are computed in two different symmetries (T_d and C_{3v}). The obtained values are (in mdyn/A): $k_{1\ \mathrm{Si\text{-}O}}(T_d)=3.75$, $k_{1\ \mathrm{Cr\text{-}O}}(T_d)=2.68$, and $k_{1\ \mathrm{Si\text{-}O}}(C_{3v})=3.83$, $k_{1_{\mathrm{Cr\text{-}O}}}(C_{3v})=2.76$. Both model symmetries show a relative percent decrease (Δ) in the Cr^{4+}-O force constant if compared to the Si-O force constant [$\Delta=(k_{1\ \mathrm{Cr\text{-}O}}-k_{1\ \mathrm{Si\text{-}O}})/k_{1\ \mathrm{Si\text{-}O}}\times 100(\%)$] of $\approx 29\%$. This decrease shows that no localized modes can exist in Cr^{4+}: Mg_2SiO_4.

2. *Estimates for $k_{Cr\text{-}O}$ and $k_{O\text{-}O}$ in T_d symmetry*

In the second approximation, using the Lagrange equations, the effective force constants can be computed for all four T_d modes from

$$k_{v2}=4k_2\ , \tag{5}$$

$$k_{v3}=k_1\left[1+\frac{4m}{3M}\right]+\frac{4k_2}{3(1+4m/3M)}\ , \tag{6}$$

$$k_{v4}=\frac{2k_2/3+2k_1(4m/3M)}{1+8m/3M}\ , \tag{7}$$

where Eq. (5) refers to $\nu_2(E)$, Eq. (6) refers to $\nu_3(T_2)$, Eq. (7) refers to $\nu_4(T_2)$. Equation (3) refers to $\nu_1(A_1)$. M is the mass of the central ion (Cr^{4+}).

By using for ν_2 a mean value of 489 cm^{-1} [$=(498+480)/2$] from Table III and Eq. (5) with $M=M_{Cr}=52$ m.u., k_2 (the effective O-O force constant) is $k_2=0.57$ mdyn/A. From Eq. (3), $\nu_1(A_1)=764$ cm^{-1} (Table III) and the above value for k_2, k_1 (the Cr^{4+}-O effective force constant) is $k_1=3.27$ mdyn/A.

Calculation of k_1 and k_2 allows an estimate of the frequencies of ν_3 [Eq. (6)] and ν_4 [Eq. (7)], and thus their assignment. With the above computed k_1 and k_2 the vibronic energies are: (a) $\nu_3(T_2)=737$ cm^{-1}. The mean measured value is 715 cm^{-1} [(740+690)/2 from Table III]; and (b) $\nu_4(T_2)=293$ cm^{-1}. The mean measured value is 272 cm^{-1} [(290+253)/2 from Table III]. Both computed values are in very good agreement with the experimental data and confirm the correctness of the mode assignments. The comparison of the Cr^{4+}-O effective force constant ($k_1=3.27$ mdyn/A) with the Si-O force constant in the RI model ($k_{1\ \mathrm{Si\text{-}O}}=3.75$ mdyn/A) still leads to a decrease of $\approx 13\%$ which shows once again that no localized modes can exist for Cr^{4+}:Mg_2SiO_4.

VII. CONCLUSION

Seven Cr^{4+} vibronic modes were obtained by means of resonance Raman scattering. These modes were measured at 253, 290, 480, 498, 690, 740, and 764 cm^{-1} in Cr^{4+}:Mg_2SiO_4. The symmetries of all of these modes have been established and correlated to the molecular (T_d) symmetry. The measured 764 cm^{-1} mode was previously reported at 770 cm^{-1}, the 498 cm^{-1} at 502 cm^{-1}, and the 740 cm^{-1} at 745 cm^{-1}.[15] It is interesting to mention that Jia *et al.*[5] observed a vibronic mode at ≈ 750 cm^{-1} in the site-selective excitation spectra of Cr^{4+}:Mg_2SiO_4 at 10 K, while Rager[16] gives a mean value of 730 cm^{-1}. Although nothing is said about the symmetry of this mode in the above-mentioned references, our study proved that the mode at 740 cm^{-1} is the strongest resonance-enhanced nontotally symmetric mode. This implies as was previously discussed in Sec. VI A that it has to vibronically couple two electronic states and would be expected to appear in an excitation spectra.

The symmetry of each of the observed resonance-enhanced modes was established and connected to their molecular symmetry (T_d) as follows: 764 cm^{-1} belongs to $\nu_1(A_1)$, 690 and 740 cm^{-1} belong to $\nu_3(T_2)$, 480 and 498 cm^{-1} belong to $\nu_2(E)$, and 253 and 290 cm^{-1} belong to $\nu_4(T_2)$. The effective Cr^{4+}-O and O-O force constants

were estimated as $k_1=3.27$ mdyn/A and $k_2=0.57$ mdyn/A, respectively. A decrease of $\approx 13-29\%$ in the value of the force constant was found for the case when Cr^{4+} substitutes for Si. This fact, together with a twofold larger Cr mass compared to Si leads to the conclusion that no Cr^{4+} localized modes exist in the crystal.

Due to the destruction of translational symmetry at the ion's site, the selection rules are relaxed. At this point the only available criterion for estimating the nonradiative decay pathway is an energetic one which is a necessary condition for phonon-vibronic mode coupling. If the vibronic mode (ν_v) is a band vibration, i.e., its energy lies in one of the lattice's allowed phonon bands and is in resonance with a phonon mode (ν_p) it strongly couples to the phonon mode ($\nu_v \rightarrow \nu_p$) leading to intense nonradiative processes and eventually loss of lasing. If the vibronic mode is a pseudolocalized vibration, i.e., its energy lies in one of the lattice's allowed phonon bands but is weakly coupled to a phonon mode, the nonradiative processes are intermediate to weak. If the vibronic mode is a localized vibration, i.e., its energy lies outside the lattice's allowed phonon bands and it cannot couple with any phonon mode. In this case its energy is transferred to multiple phonons (at least two phonon modes ν_{p1} and ν_{p2}, $\nu_v \rightarrow \nu_{p1}+\nu_{p2}$). The coupling is weak leading to weak nonradiative processes. The probability of any of the above described processes is determined by its order. Band vibrations necessary involve first-order (strong, $\nu_v \rightarrow \nu_p$) nonradiative processes while localized vibrations necessary involve second or higher order (weak, $\nu_v \rightarrow \nu_{p1}+\nu_{p2}+\cdots$) nonradiative processes. Pseudolocalized vibrations can involve both first- and higher-order nonradiative processes.

The first step in the process of energy transfer from the excited ion into the lattice through nonradiative processes is mediated by the ion's vibronic modes. The resonance Raman technique allows for their identification in terms of symmetry and energy. The energy of the vibronic modes gives information regarding the type of nonradiative processes to be expected in a lasing crystal. Figures 2 and 3 together with the conclusion in Sec. VI C of the text show that Cr^{4+}:Mg_2SiO_4 supports only pseudolocalized vibrations leading to intermediate to weak nonradiative processes. The same conclusion is drawn from the relative small change in phonon population (peak intensity) for the investigated phonon modes as a function of pump-probe time delay.[1]

A candidate for a first-order process (with the appropriate band width, as is the case in time-resolve experiments[1]) is the 253 cm^{-1} vibronic mode decaying into the 225 cm^{-1} phonon mode. The case of second-order processes is illustrated by the 764 cm^{-1} vibronic mode decaying into the 335 and 424 cm^{-1} phonon modes and the 740 cm^{-1} vibronic mode decaying into two 370 cm^{-1} phonon modes. All the above-mentioned phonon modes (except for the 424 cm^{-1} which is weak) were shown to be involved in nonradiative processes following photoexcitation in Cr^{4+}:Mg_2SiO_4.[1] This work is a step in the process of connecting impurity-associated modes to lattice modes in order to establish criteria which enable energy transfer between vibronic and phonon modes in nonradiative processes.

ACKNOWLEDGMENTS

We wish to thank Dr. N. Ockman for helpful discussions and the Army Research Office for support.

[1] S. G. Demos, J. M. Buchert, and R. R. Alfano, Appl. Phys. Lett. **61**, 660 (1992).

[2] V. Petričević, S. K. Gayen, and R. R. Alfano, Appl. Phys. Lett. **53**, 2590 (1988).

[3] V. Petričević, S. K. Gayen, and R. R. Alfano, in *OSA Proceedings on Tunable Solid State Lasers,* edited by M. L. Shand and H. P. Jenssen (Optical Society of America, Washington D.C., 1989), Vol. 5, p. 77.

[4] H. R. Verdun, L. M. Thomas, D. M. Andrauskas, T. McColum, and A. Pinto, Appl. Phys. Lett. **53**, 2593 (1988).

[5] W. Jia, H. Liu, S. Jaffe, W. M. Yen, and B. Denker, Phys. Rev. B **43**, 5234 (1991).

[6] Y. Yamaguchi, K. Yamagishi, A. Sugimoto, and Y. Nobe, in *OSA Proceedings on Advanced Solid-State Lasers,* edited by G. Dube and L. Chase (Optical Society of America, Washington D.C., 1991), Vol. 10, p. 52.

[7] B. H. T. Chai, Y. Shimony, C. Deka, X. X. Zhang, E. Munin, and M. Bass, in *OSA Proceedings on Advanced Solid-State Lasers,* edited by L. L. Chase (Optical Society of America, Washington D.C., 1992), Vol. 13, p. 28; A. A. Kaminskii, B. V. Mill, E. L. Belokoneva, and A. V. Butashin, Inorg. Mater. **27**, 1899 (1991).

[8] K. K. Rebane, *Impurity Spectra of Solids* (Plenum, New York, 1970).

[9] V. Devarajan and E. Funck, J. Chem. Phys. **62**, 9 (1975).

[10] *Internationale Tabellen zur Bestimmung von Kristalstrukturen* (Gebrüder Borntraeger, Berlin, 1944).

[11] K. Iishi, Am. Mineral. **63**, 1198 (1978).

[12] W. G. Fateley, F. R. Dolish, N. T. McDevitt, and F. F. Bentley, *Infrared and Raman Selection Rules for Molecular and Lattice Vibrations* (Wiley Interscience, New York, 1972).

[13] A. C. Albrecht, J. Chem. Phys. **43**, 5 (1961).

[14] H. Hamaguchi, Adv. Infrared Raman Spectroscopy **12**, 273 (1985).

[15] S. G. Demos, Ph.D. thesis, CUNY, 1993.

[16] H. Rager and G. Weiser, Bull. Mineral. **104**(4), 603 (1981).